Published in: European Journal of Neuroscience (2002), vol. 16, pp. 2324-2332
Status: Postprint (Author's version)

Vasopressin and oxytocin reverse adenosine-induced pituicyte stellation via calcium-dependent activation of Cdc42

Lia Rosso,[1] Brigitta Peteri-Brunbäck,[1] Valérie Vouret-Craviari,[2] Christophe Deroanne,[2] Ellen Van Obberghen-Schilling[2] and Jean-Marc Mienville[1]

[1]*CNRS-UMR 6548, Laboratoire de Physiologie Cellulaire et Moléculaire, Université de Nice-Sophia Antipolis, Nice, France*

[2]*CNRS-UMR 6543, Centre Antoine Lacassagne, Université de Nice-Sophia Antipolis, Nice, France*

Abstract

In view of the potential impact of pituicyte morphology on neurohypophysial hormone secretion, we have studied the mechanisms involved in the shape changes induced by vasopressin (AVP) and oxytocin (OXT) in cultured rat pituicytes. Pituicytes induced to become stellate in the presence of 10 μM adenosine revert to their nonstellate shape ~20 min after application of AVP or OXT. The IC_{50} for this effect is 0.1 nM for AVP and 36 nM for OXT. Both agonists induce Ca^{2+} signals in pituicytes, comprised of a transient peak and a plateau phase that is dependent on the presence of extracellular Ca^{2+}. The EC_{50} values of AVP for the transient and sustained responses are 4.5 and 0.1 nM, respectively; corresponding values for OXT are 180 and 107 nM. We determined pharmacologically that these hormone-induced Ca^{2+} signals are mediated by the V_{1a} subtype of vasopressin receptors, similar to what we previously observed for hormone-induced reversal of stellation. Removal of extracellular Ca^{2+} or chelation of intracellular Ca^{2+} partially prevented AVP from reversing stellation, suggesting a role for Ca^{2+} in this event. We previously established that adenosine-induced stellation of pituicytes occurs via RhoA inhibition. However, pharmacological experiments and pull-down assays presented here show that AVP-induced reversal of stellation does not involve RhoA activation. Rather, AVP was found to induce a time-dependent activation of Cdc42, another small GTPase involved in cytoskeletal plasticity. Activation of Cdc42 by AVP is sensitive to intra- and extracellular Ca^{2+} depletion, similar to AVP-induced reversal of stellation. Furthermore, AVP-induced reversal of stellation is blocked by expression of an NWASP fragment known to inhibit endogenous Cdc42.

Keywords : cytoskeleton ; glia ; neurohypophysis ; rat ; RhoA

Introduction

Two main classes of receptor-specific activators are known to induce neurohypophysial astrocyte (pituicyte) stellation *in vitro.* These include β-adrenergic agonists, which stimulate cAMP production (Bicknell *et al.,* 1989), and purinergic agonists, the transduction pathway of which is only partially elucidated (Miyata *et al.,* 1999; Rosso *et al.,* 2002). A potentially common downstream mechanism mediating pituicyte stellation is inhibition of RhoA (Rosso *et al.,* 2002), a monomeric GTPase known to be involved in cytoskeletal reorganization (Machesky & Hall, 1996). The physiological relevance of these findings is that pituicyte stellation *in vitro* is likely to correspond to morphological changes that occur *in vivo* in these same cells during specific physiological conditions such as lactation and dehydration. Furthermore, these morphological changes are believed to facilitate and amplify secretion of the neurohypophysial hormones vasopressin (AVP) and oxytocin (OXT) (reviewed by Theodosis & MacVicar, 1996; Hatton, 1999). Relevant to the purinergic pathway, it has been shown that ATP, which is present in most secretory vesicles (Gratzl *et al.,* 1980; Zimmermann, 1994), is co-released with these hormones from neurohypophysial terminals (Sperlágh *et al.,* 1999). In our previous studies (Rosso *et al.,* 2002), we showed that ATP induces pituicyte stellation through its metabolism to adenosine, most likely owing to the presence of ecto-ATPases on the outer surface of pituicytes (Thirion *et al.,* 1996). We also demonstrated that adenosine-mediated stellation is transduced via Al receptor activation, followed by RhoA inhibition and subsequent depolymerization of actin stress fibers. The coupling mechanism linking Al receptor stimulation to RhoA inhibition is less clear, though we have already ruled out involvement of intracellular Ca^{2+} ($[Ca^{2+}]_i$), or mitogen-activated protein kinase (MAPK) pathways (Rosso *et al.,* 2002).

Hatton (1988, 1999) hypothesized that changes in pituicyte morphology might facilitate neurohypophysial hormone secretion. With respect to the purinergic pathway, this would imply a self-amplifying loop mechanism whereby co-released ATP would further enhance secretion through its (adenosine-mediated) morphogenic effects on pituicytes. It is therefore straightforward to postulate that some sort of negative feedback process might participate in the homeostatic control of hormone secretion. Indeed, in the course of our previous work (Rosso *et al.,* 2002), we found that AVP and OXT acting at V_{1a} receptors effectively reversed adenosine-induced pituicyte stellation. In the present work, we sought to: (i) quantify hormone-induced reversal of stellation; and (ii), examine the potential pathways transducing this effect. We found that AVP reverses stellation at physiologically relevant concentrations, whereas OXT mimics this effect at much higher concentrations. The novel and intriguing aspect of our results resides in the fact that the diametrical effects of adenosine and AVP on pituicyte stellation are mediated by distinct and apparently independent transduction pathways. Whereas adenosine acts independently of Ca^{2+} via RhoA inhibition, AVP induces Ca^{2+}-dependent stimulation of yet another cytoskeletal modulating GTPase, Cdc42.

Materials and methods

Pituicyte explant cultures

Adult Wistar rats (150-200 g) were anaesthetized with CO_2 and decapitated in accordance with French/European ethical guidelines. For each culture, 4-6 hypophyses were placed in Hank's balanced salt solution (Gibco) supplemented with 10 mM HEPES, 0.5 mg/mL BSA, 100 U/mL penicillin and 100 µg/mL streptomycin. The posterior lobe was separated from the anterior and intermediate lobes under a dissecting microscope, and divided into ~20 pieces. For morphological and calcium studies, each piece of tissue was placed in a 35-mm plastic dish coated with 0.05 mg/mL collagen and containing DMEM medium (Gibco) supplemented with 1.2 g/l $NaHCO_3$ and 10% foetal calf serum. For RhoA and Cdc42 assays, five tissue pieces were plated in 60 mm dishes. Cultures were maintained at 37 °C in an incubator supplied with a 5% CO_2/95% air humidified atmosphere. The medium was replaced every 2-3 days. All experiments were performed on cell cultures after 8-12 days *in vitro,* at which time a monolayer of pituicytes had spread 5-10 mm from the explant. Control experiments (n = 10) performed as previously published by this laboratory (Troadec *et al.,* 1999) revealed that > 95% of the cells were GFAP-positive.

Morphological analysis

Because of the inhibitory effect of serum on stellation, cells were switched to 0.025% serum medium 1 h before the experiments, a standard procedure followed by several authors (e.g. Bicknell *et al.,* 1989; Ramsell & Cobbett, 1997). This preconditioning was followed by a 70 min treatment (37 °C) with adenosine with or without the membrane-permeable calcium chelator BAPTA-AM. AVP and OXT were applied for 20 min, 50 min after adenosine addition, i.e. at the time of maximum induction of stellation by adenosine (see Results). Image acquisition was performed with a digital still camera and Adobe Photoshop software for cell counting. Digitized images were given a coded file name with respect to treatment in order to perform blind counting. Cells were considered as stellate when they displayed ≥2 processes (Ramsell & Cobbett, 1997). For each culture dish, the proportion of stellate cells was assessed by counting 100-200 cells at 10 × magnification over five arbitrarily chosen areas 0.9 × 0.7 mm wide, and taking the resulting average (Rosso *et al.,* 2002).

Data are presented as mean ± SEM, and the number on top of each bar represents the number of culture dishes counted. Differences between treatment groups were evaluated with analysis of variance followed by a Bonferroni *post hoc* test with significance set at $P < 0.05$.

Calcium imaging

Intracellular Ca^{2+} ($[Ca^{2+}]_i$) was measured with the ratiometric, membrane-permeable, fluorescent probe Fura-2 AM. Briefly, pituicyte cultures were incubated for 45 min at 37 °C in the presence of 5 µM Fura-2 AM + 0.01% pluronic acid (+ 10 µM adenosine to induce stellation). During experiments, culture dishes were continuously superfused with Ringer solution (3 mL/min). These experiments were performed on the stage of an inverted microscope (Zeiss ICM 405) equipped with a Xenon lamp and a rotating filter set allowing 350/380 nm excitation. Axon Imaging Workbench 2.2 software was used to drive the filter wheel, acquire fluorescence images and process data. For any given experiment, fluorescence signals were averaged from 15-20 cells defined as 'regions of interest'. Free $[Ca^{2+}]_i$ was estimated from a calibration procedure using a 'zero-Ca' solution (3 mM EGTA + 2 µM ionomycin) and a Ca-saturated solution (3 mM $CaCl_2$ + 2 µM ionomycin). The F350/ 380 ratios were converted to free $[Ca^{2+}]_i$ using the Grynkiewicz equation (see Hatton *et al.,* 1992). Drugs were applied

locally through a miniperfusion system.

RhoA and Cdc42 GTPase activity assay

Assays for GTPase were performed using five 60 mm culture dishes for each experimental condition (see details in the Results). The cells were lysed in buffer A (25 mM HEPES pH 7.3, 150 mM NaCl, 5 mM $MgCl_2$, 0.5 mM EGTA, 0.5% Triton X-100, 4% glycerol, 20 mM β-glycerophosphate, 10 mM NaF, 2 mM Na-orthovanadate, 5 mM dithiothreitol and protease inhibitors) for 10 min at 4 °C; the Triton X-100 insoluble material was removed by centrifugation (10 min; 9000 *g*), and the lysates were incubated for 30 min at 4 °C with 20 μg bacterially produced GST-RBD (glutathione-S-transferase-RhoA binding domain from Rhotekin; Ren *et al.,* 1999) or GST-CRIB (Cdc42/Rac interactive binding domain from PAK; Bagrodia *et al.,* 1995), which were bound to glutathione-coupled Sepharose beads. Beads were washed four times in buffer A, resuspended in Laemmli buffer, and proteins were separated by SDS-PAGE on 12% acrylamide gels. RhoA and Cdc42 were detected by Western blotting using specific antibodies (RhoA 26C4: *sc-418*, Santa Cruz Biotechnology; monoclonal anti-cdc42, BD Biosciences). Before incubation with the beads, 50 μL aliquots were removed from each sample for determination of total GTPase content. The latter was used to quantify GTPase activation by densitometric analysis. The optical density of each band on any given Western blot was analysed with PCBAS software (Raytest, Straubenhardt, Germany). After background subtraction, the ratio of activated/total GTPase was then calculated and normalized to the lowest ratio value found in the blot.

Cell transfection and immunofluorescence

For immunofluorescence experiments, pituicytes were plated on 18 mm-diameter glass coverslips placed in 35 mm culture dishes. Using the calcium phosphate precipitation method, pituicytes were transfected with a Myc-tagged pcDNA3 plasmid expressing the Cdc42 GTPase binding domain (GBD) of NWASP, a Wiscott-Aldrich syndrome protein (WASP)-related protein (material provided by A. Hall, University College, London, UK, and P. Roux, CNRS UPR 1086, Montpellier, France). After sequential exposure to adenosine and AVP, cells were fixed with 3% paraformaldehyde + 2% sucrose at 37 °C for 15 min, washed 3 times in PBS, permeabilized for 5 min in PBS + 0.2% Triton, rinsed three times in PBS, and saturated 15 min with 3% bovine serum albumin. Cells were then incubated overnight at 4 °C with polyclonal anti-Myc antibody (MBL, Nagoya, Japan; diluted 1 : 1000) in order to distinguish transfected from nontransfected cells. After three more rinses in PBS, antirabbit, FITC-coupled secondary antibody diluted 1 : 100 was applied for 1 h at room temperature. Actin filaments were labelled simultaneously with Rhodamin-coupled phalloidin (Sigma; 67 ng/mL). After rinsing in phosphate-buffered saline, coverslips were mounted on slides in the presence of Citifluor for observation on an epifluorescence microscope.

Drugs

Adenosine, AVP, OXT, bradykinin and BAPTA-AM were purchased from Sigma; the following compounds were given to us by the indicated persons: SR 49059 ((2S) 1-[(2R 3S)-5-chloro-3-(2-chlorophenyl)-1-(3,4-dimethoxybenzene-sulphonyl)-3-hydroxy-2,3-dihydro-1H-indole-2-carbonyl]-pyrrolidine-2-carboxamide) and SR 121463 (1-[4-(N-tert-butylcarbamoyl)-2-methoxybenzene sulphonyl]-5-ethoxy-3-spiro-[4-(2-morpholinoethoxy)cyclohexane]indoline-2-one) from C. Serradeil-Le Gal (Sanofi-Synthélabo, Toulouse, France); CL 12-27 ([1-deamino-4-cyclohexylalanine] arginine vasopressin) and $d(CH2)_5[Tyr(Me)^2,Thr^4,Tyr\text{-}NH_2^9]$OVT (dOT) from M. Manning (Medical College of Ohio, Toledo, USA); Y-27632 ((+)-(R)-*trans*-4-(1-aminoefhyl)-N-(4-pyridyl)cyclohexane-carboxamide) from A. Yoshimura (Yoshitomi Pharmaceutical Industries, Osaka, Japan); C3 toxin from P. Boquet (INSERM U-452, Nice, France). None of the solvents at the maximal concentrations used had any effect on pituicytes (≤ 5% stellation).

Results

AVP and OXT-mediated reversal of adenosine-induced pituicyte stellation

Consistent with our previous work, adenosine induced marked stellation in a vast majority of pituicytes, with a maximal effect after 30-70 min of treatment (Fig. 1A and B). In the continued presence of agonist, cells spontaneously reverted to their basal fusiform morphology within approximately 2 h, perhaps as a result of agonist catabolism or receptor desensitization. However, when we added AVP or OXT 50 min after adenosine, i.e. around the peak of its effect, reversal of stellation was achieved within about 20 min (Fig. 1C and D). We then investigated the concentration dependence of AVP- and OXT-induced reversal of stellation. The data summarized in the graph of Fig. 2 reveal an 'IC_{50}' of 0.1 nM for AVP and 36 nM for OXT. These values are

Published in: European Journal of Neuroscience (2002), vol. 16, pp. 2324-2332
Status: Postprint (Author's version)

reasonably close to the binding K_D of AVP and OXT to V_{1a} receptors (0.8 and 146 nM, respectively; Andres *et al.,* 2002), which is consistent with our previous finding that V_{1a} receptors mediate the morphogenic effects of both hormones (see fig. 8 in Rosso *et al.,* 2002). In parallel, we examined whether OXT might also act on its own receptors. However, 100 nM dOT, a specific OXT receptor antagonist (Elands *et al.,* 1988), did not prevent OXT-induced reversal of stellation [11.2 ± 2.7% vs. 16.1 ± 3.3% stellation in the absence (n = 5) and presence (n = 9) of dOT; P = 0.17]. This result confirms our previous finding that the effects of both AVP and OXT are exerted exclusively through V_{1a} receptors.

FIG. 1. *Morphogenic effects of adenosine, AVP and OXT on rat cultured pituicytes. Digital microphotographs (500 × 500 µm) were taken in control conditions (A; 0.025% serum), and after a 70 min treatment with 10 µM adenosine alone (B), or in the presence of 1 nM AVP (C), or 100 nM OXT (D) added 50 min after adenosine.*

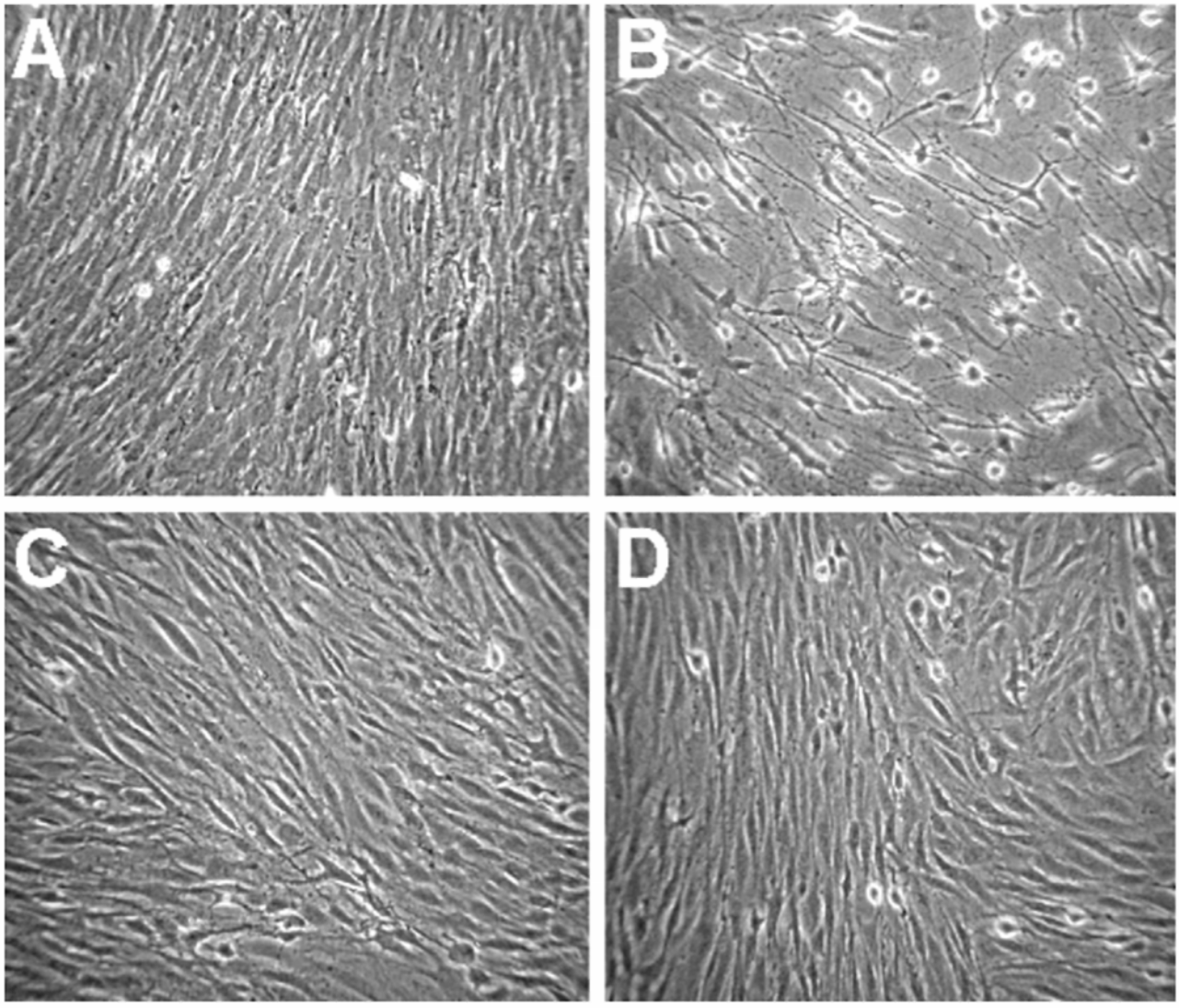

Published in: European Journal of Neuroscience (2002), vol. 16, pp. 2324-2332
Status: Postprint (Author's version)

FIG. 2. *Dose-dependence of AVP- and OXT-induced reversal of pituicyte stellation. The protocol used is as described in Methods, i.e. 50 min of adenosine (10 µM) treatment followed by 20 min of adenosine + different concentrations of hormone. Each data point is the mean ± SEM of 3-6 culture dishes. Data were fitted with a logistic equation of the form: $S = \{S_{max} - (S_{max}\,[H])/(IC_{50} + [H])\} + S_{min}$, where S and S_{max} are percentage stellation and its maximum, S_{min} is a residual stellation present in control conditions (see Rosso et al., 2002), [H] is hormone concentration, and IC_{50} is the hormone concentration that reverses 50% of S_{max}.*

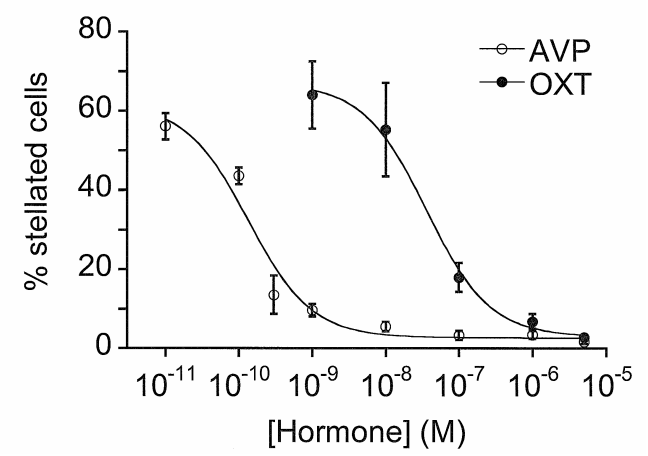

FIG. 3. *Cytosolic calcium ($[Ca^{2+}]_i$) signals induced by AVP and OXT in pituicytes. AVP (A and C) and OXT (B) produced similar $[Ca^{2+}]_i$ signals though at concentrations two orders of magnitude apart, whereas CL 12-27 (C) failed to elicit any effect. (D) The OXT response displayed in B is reproduced here after normalization (as percentage of maximum fluorescence) so as to scale it to another superimposed response to 1 µM OXT in the absence of external Ca^{2+} (+ 1 mM EGTA). Qualitatively similar results were obtained with 100 nM AVP.*

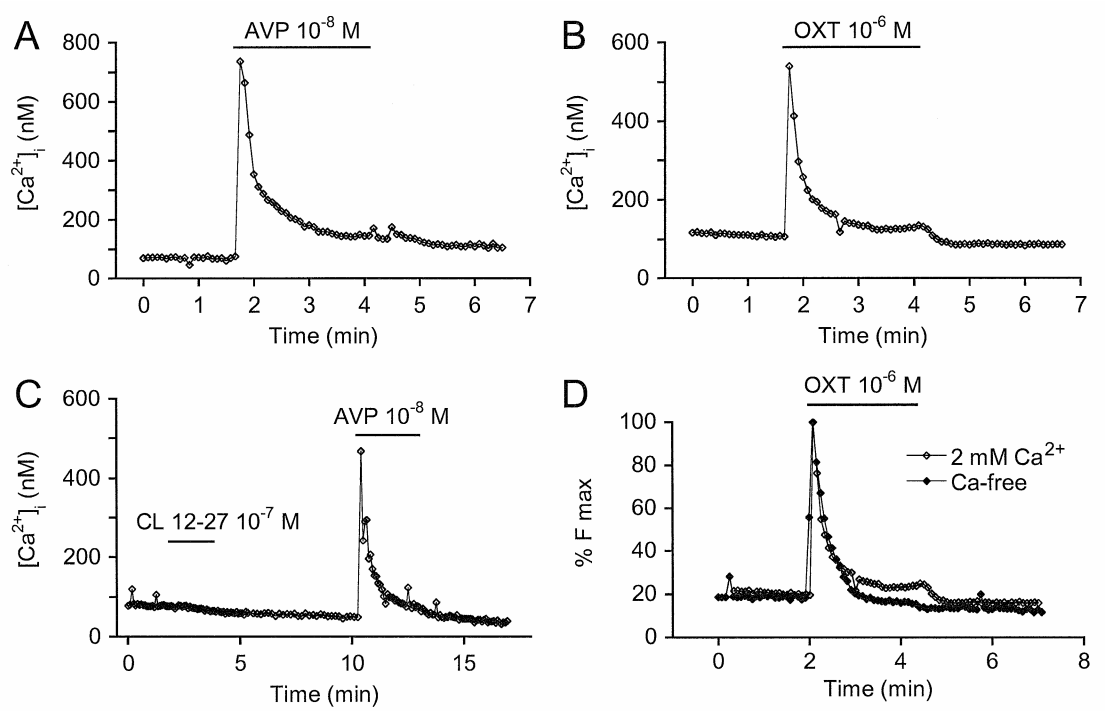

Published in: European Journal of Neuroscience (2002), vol. 16, pp. 2324-2332
Status: Postprint (Author's version)

Calcium signals induced by AVP and OXT

Vasopressin and OXT have been shown to mobilize $[Ca^{2+}]_i$ in pituicytes (Hatton *et al.,* 1992). To investigate whether this could be a signalling pathway involved in hormone-induced reversal of stellation, we first confirmed that both AVP (10 nM) and OXT (1 μM) were able to reliably evoke a strong $[Ca^{2+}]_i$ signal in our pituicyte cultures (Fig. 3A-C). At these relatively high doses, the response was generally biphasic with a main component, i.e. the fast transient, that was independent of external Ca^{2+}, and a small sustained component that was eliminated in Ca-free medium (Fig. 3D). This latter component, corresponding to Ca^{2+} entry through plasma membrane channels, could occur in the absence of any transient (see the foot of the dose-response curves for AVP in Fig. 4A), which would tend to exclude involvement of store-dependent, capacitive Ca^{2+} entry. At low concentrations (1 nM), AVP often triggered virtually pure sustained responses, which were not affected by nifedipine, ω-conotoxin or La^{3+} (not shown). This appears to rule out activation of voltage-dependent Ca^{2+} channels by AVP, consistent with the absence of such channels in pituicytes (Hatton *et al.,* 1992).

This leaves the possibility that the sustained response could be mediated by store-independent, receptor-operated Ca^{2+} channels of the transient receptor potential type, which have recently been shown to be activated by AVP (Jung *et al.,* 2002).

Next, we established dose-response curves for the different phases of the Ca^{2+} signals induced by AVP and OXT. Analysis of transient peak amplitude resulted in an EC_{50} of 4.5 nM for AVP and 180 nM for OXT, whereas that of sustained responses yielded an EC_{50} of 0.1 nM for AVP and 107 nM for OXT (Fig. 4A). These dose-response curves are similar to those established for hormone-induced reversal of stellation, particularly with respect to their concentration span and differences in potency between the two hormones (compare Figs 2 and 4A). Interestingly, the IC_{50} of AVP for reversal of stellation (0.1 nM) is identical to its EC_{50} for eliciting the sustained component of the Ca^{2+} signal.

Finally, we studied the receptor subtype specificity of hormone-induced Ca^{2+} responses. CL 12-27, an agonist of the V_{1b} subtype of AVP receptors (Derick *et al.,* 2001), failed to elicit any Ca^{2+} signal (Fig. 3C; $n = 3$), thus excluding involvement of V_{1b} receptors; V2 receptors were also ruled out because SR 121463, a specific V2 antagonist (Serradeil-Le Gal, 1998), failed to affect AVP responses (Fig. 4B). In contrast, SR 49059, a specific antagonist of the V_{1a} receptor subtype (Serradeil-Le Gal, 1998), substantially reduced Ca^{2+} signals elicited by 100 nM AVP, and virtually abolished those elicited by 30 nM AVP (Fig. 4B). Also, 100 nM SR 49059 completely abolished Ca^{2+} responses induced by 0.1 and 1 μM OXT ($n = 2$; not shown). This pharmacological profile is identical to the one we found for AVP- and OXT-mediated reversal of stellation (Rosso *et al.,* 2002). Taken together, these data suggest that a Ca^{2+} signal is involved in V_{1a} receptor-mediated reversal of adenosine-induced stellation.

To test this hypothesis, we performed morphological experiments in conditions of intracellular and/or extracellular Ca^{2+} depletion by incubating pituicytes with the membrane permeable Ca^{2+} chelator BAPTA-AM (10 μM added at the same time as adenosine), and/or removing extracellular Ca^{2+} (+ 1 mM EGTA). Results are summarized in Fig. 5. From statistical analysis of these results, we can infer the following: (i) depleting free $[Ca^{2+}]_i$ and/or $[Ca^{2+}]_e$ did not interfere with adenosine-induced stellation (compare 1 st with 3rd, 6th and 8th bars from the left); (ii) $[Ca^{2+}]_i$ chelation did antagonize AVP-induced reversal of stellation (compare 2nd and 4th bars); and (iii), this effect was incomplete (compare 3rd and 4th bars) and was not different from that elicited by $[Ca^{2+}]_e$ depletion or a combination of both (compare 4th, 7th and 9th bars). Therefore, AVP-induced reversal of stellation involves a Ca^{2+} signal, whether the ion be of intracellular or extracellular origin, but the inhibitory effects of $[Ca^{2+}]_i$ and $[Ca^{2+}]_e$ depletion are not additive. Fura-2 experiments allowed us to verify that the latter conditions (i.e. 0 Ca + EGTA + BAPTA) prevented the generation of any Ca^{2+} signal by AVP ($n = 3$; not shown). From this we conclude that the action of Ca^{2+} is only permissive as its complete blockade antagonizes less that 100% (i.e. ~70%) of the effect of AVP on stellation reversal.

Published in: European Journal of Neuroscience (2002), vol. 16, pp. 2324-2332
Status: Postprint (Author's version)

FIG. 4. *Pharmacology of calcium signals elicited in pituicytes by AVP and OXT. (A) Dose-response relationships of peak and plateau components of Ca^{2+} signals vs. hormone concentration. The plateau was estimated after subtracting baseline from the end of the signal, whereas the peak corresponds to the amplitude difference between the beginning and the end of the signal. Data were fitted with a Michaelis-Menten equation of the form: $C = (C_{max} \times [H])/(EC_{50} + [H])$, where C and C_{max} are the Ca^{2+} response and its maximum, [H] is hormone concentration, and EC_{50} is the hormone concentration that elicits 50% of C_{max}. (B) Effects of 100 nM SR 49059 or SR 121463 on Ca^{2+} responses mediated by 30 or 100 nM AVP (as indicated in brackets). In this case, total amplitude (peak + plateau) of the Ca^{2+} signal was measured after pre- and coapplication of antagonist, and normalized to control amplitude in AVP alone. For both (A and B), each data point is the mean ± SEM of 3-4 experiments × 15-20 cells per experiment.*

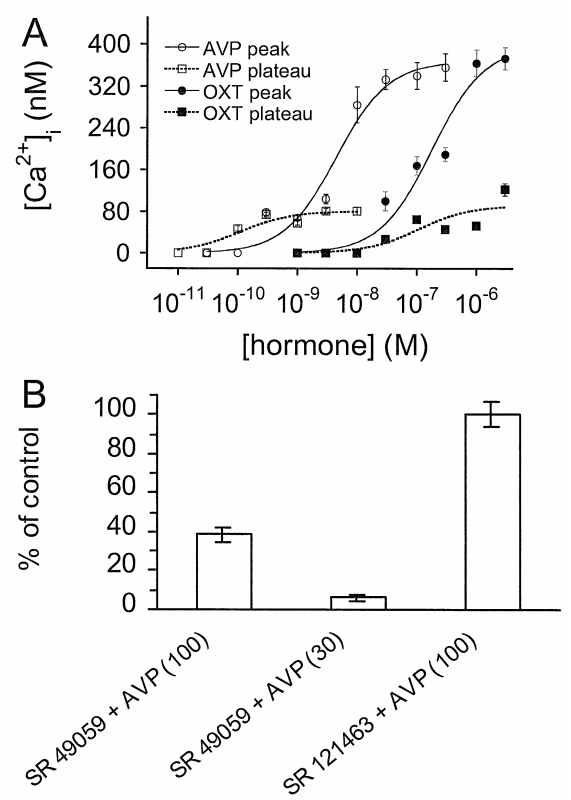

FIG. 5. *Calcium dependence of AVP-mediated reversal of adenosine-induced pituicyte stellation. Cells were incubated with adenosine (Ado; 10 µM) with or without BAPT A-AM (10 µM) or AVP (10 nM) in regular or Ca^{2+}-free (0 Ca; supplemented with 1 mM EGTA) culture medium. *Significantly different from BAPTA + Ado + AVP.*

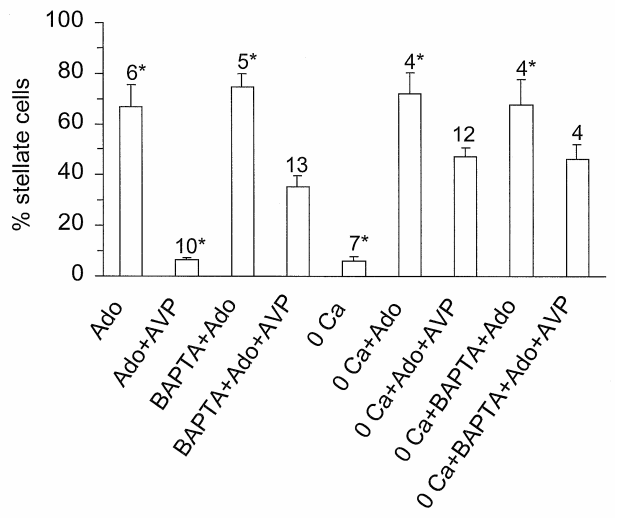

FIG. 6. *Pathways involved in reversal of RhoA-related pituicyte stellation. The treatment protocol for induction of stellation with Y-27632 (7 µM) or adenosine (10 µM; Ado) and its reversal by lysophosphatidic acid (10 µM; LPA) or bradykinin (100 nM; BK) was the same as that used previously, i.e. 50 min with stellation inducers followed by an additional 20 min with reversal inducers (see Methods). C3 toxin (20 µg/mL) was applied for 16 h because of its poor membrane penetration, which appears to result in a somewhat lesser amount of stellation than that observed with either adenosine (see Fig. 5) or Y-27632. Lysophosphatidic acid (10 µM) or AVP (10 nM) were subsequently applied for 20 min * Significantly different from C3.*

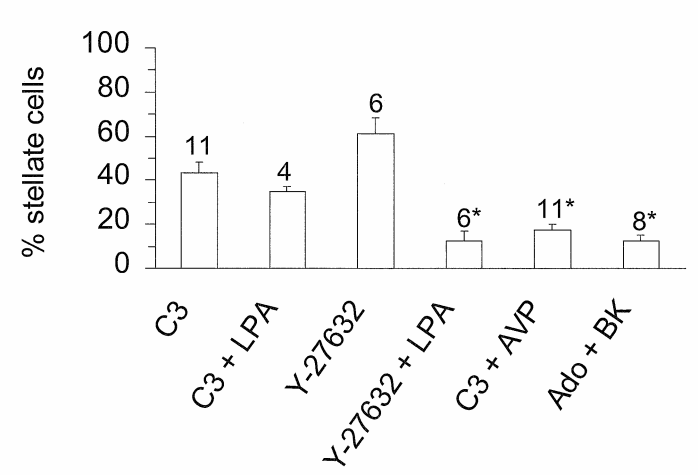

Role of RhoA and Cdc42 in reversal of stellation

On the basis of our previous finding that adenosine induces stellation through RhoA inhibition, we tested whether reversal of this effect by AVP might involve RhoA activation. This hypothesis was initially weakened by the fact that AVP was able to reverse stellation induced by C3 transferase (Fig. 6), a *Clostridium botulinum* toxin that covalently modifies and inhibits RhoA (Chardin *et al.,* 1989; Machesky & Hall, 1996). Indeed, RhoA inhibition by C3 seems insurmountable because lysophosphatidic acid (LPA), a powerful RhoA activator that prevents adenosine-induced stellation (Rosso *et al.,* 2002), failed to reverse C3-induced stellation (Fig. 6). However, LPA (as well as AVP; data not shown) was able to reverse the effect of Y-27632 (Fig. 6), a specific inhibitor of p160Rho kinase, a downstream effector of RhoA (Uehata *et al.,* 1997). This suggests that at least one other RhoA effector is involved in cytoskeletal changes (Machesky & Hall, 1996), which is discussed further below.

Conclusively ruling out RhoA involvement in stellation reversal by AVP, our pull-down experiments showed that the hormone failed to relieve adenosine-mediated RhoA inhibition, whereas LPA used as a control did restore a detectable level of activated RhoA (Fig. 7A and B). We therefore hypothesized that hormone-induced reversal of stellation might be mediated through another Rho-family GTPase such as Cdc42, which is known to mediate formation of bradykinin-stimulated membrane protrusions (Lim *et al.,* 1996; Machesky & Hall, 1996). Indeed, we found that bradykinin was able to reverse adenosine-induced stellation (compare first bar of Fig. 5 with last bar of Fig. 6). This prompted us to perform pull-down assays that clearly demonstrated time-dependent activation of Cdc42 by AVP up to a level similar to that obtained with bradykinin (Fig. 7C).

A straightforward question that arose next concerned a possible link between AVP-induced Ca^{2+} signals and Cdc42 activation, inasmuch as bradykinin is a powerful Ca^{2+} mobilizing agent in pituicytes (Rosso *et al.,* 2002). If a causal link did exist between these two events, what might be their sequential chronology? Intuitively, it seems that the Ca^{2+} signal, which is rather fast (Fig. 3A), should precede Cdc42 activation, which can develop over a time frame of several minutes (Fig. 7C). In order to check whether Cdc42 activation by AVP was Ca^{2+}-dependent, we performed pull-down assays in cells treated to eliminate Ca^{2+} on either side of the membrane (0 Ca + EGTA + BAPTA-AM). The results shown in Fig. 7C (last lane) and D clearly indicate that in these conditions AVP failed to activate Cdc42.

So far, our data show a good correlation between Cdc42 activation and reversal of pituicyte stellation by AVP, but a causal relationship between the two events remains to be established. In order to demonstrate that the morphogenic effects of AVP are coupled to Cdc42 activation, we transfected pituicytes with a pcDNA3 plasmid expressing the Cdc42 GTPase binding domain of NWASP (NWASP-GBD), which is known to inhibit endogenous Cdc42 activity (Philips *et al.,* 2000). These cells were then challenged with adenosine followed by

AVP in the usual conditions. Despite a low transfection yield, we observed that all transfected cells (*n* = 14 anti-Myc-positive cells in three culture dishes) remained stellate, whereas stellation was reversed in neighbouring nontransfected cells (Fig. 8). As NWASP-GBD expression *per se* had no effect on cell morphology (not shown), these results clearly indicate that AVP fails to reverse pituicyte stellation when Cdc42 is blocked.

FIG. 7. *RhoA and Cdc42 activity detected in pituicytes by pull-down experiments performed in the various conditions indicated. (A) RhoA activity is inhibited by adenosine (10 µM for 45 min; Ado), remains suppressed upon subsequent addition of AVP (10 nM for 5 min), but is restored by the addition of LPA (10 µM for 5 min). (B) Summary of results obtained from 3 RhoA pull-downs (mean ± SEM). (C) Cdc42 activity is increased by AVP in a time-dependent manner (2 vs. 5 min exposure), and by bradykinin (BK) used as a standard activator. In conditions of both extra- and intracellular Ca^{2+} depletion, Cdc42 activity is not increased by AVP. (D) Summary of results obtained for 5 min stimulation with AVP with or without Ca^{2+} (mean ± SEM of three Cdc42 pull-downs). In (B and D), optical density (OD) of GTPase signal is expressed in arbitrary units established as described in Materials and Methods. *Significantly different from Ado at $P < 0.05$ (ANOVA followed by Bonferroni's post hoc test).*

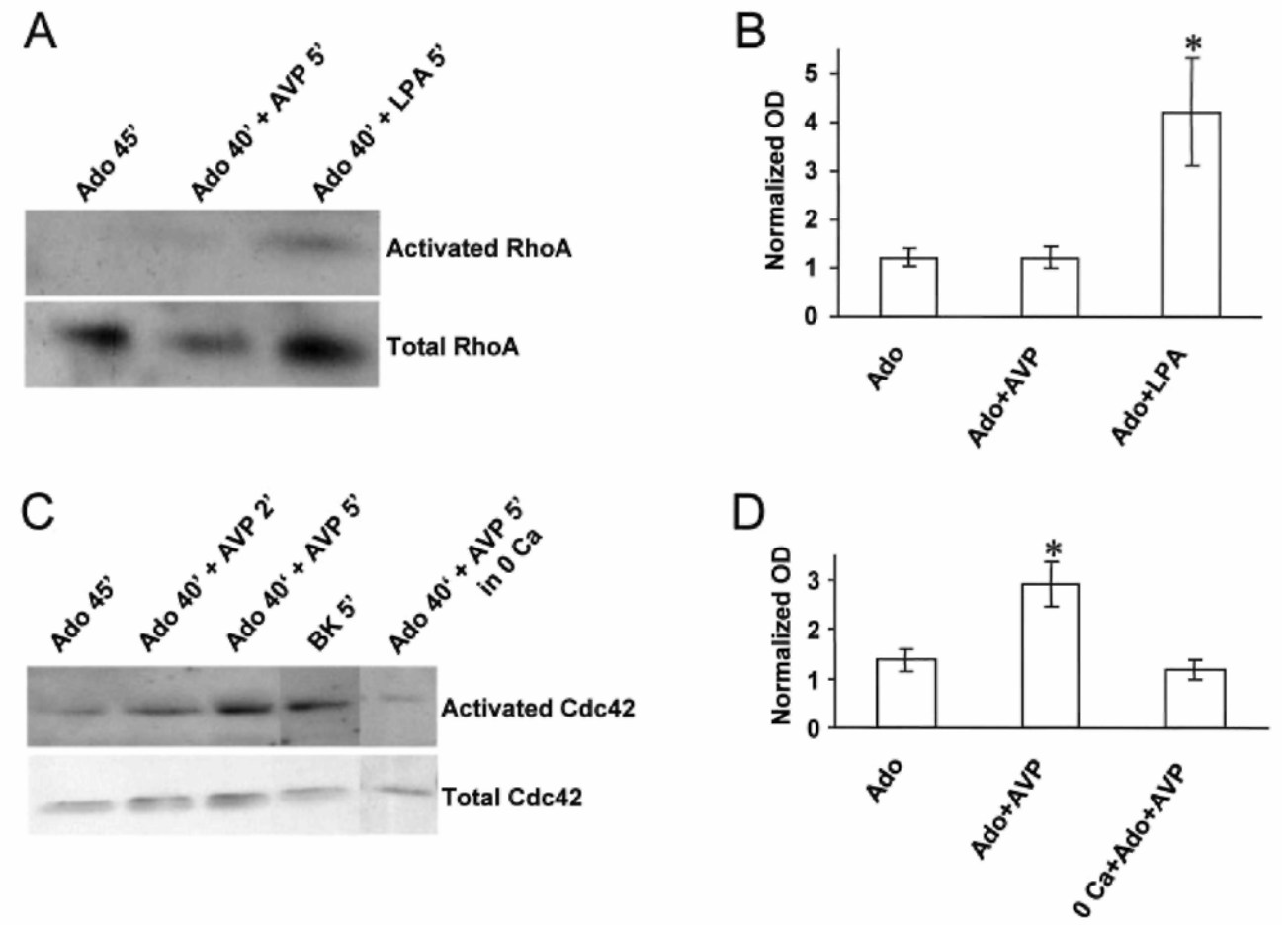

FIG. 8. *Blockade of pituicyte stellation reversal by NWASP-GBD. Microphotographs show fluorescent labelling of F-actin (A and B), anti-Myc antibody indicative of NWASP-GBD transfection (C and D), and double-labelling overlays of both labels (E and F). Cells were first made stellate with 10 µM adenosine, and then exposed to 10 nM AVP. Anti-Myc labelling (C) shows only two cells likely to express NWASP-GBD, both of which remained stellate. Stellation of the lower cell is further shown by right panel enlargements corresponding to white boxes in left panels. Scale bar 70 µm (A, C and E); 30 µm (B, D and F).*

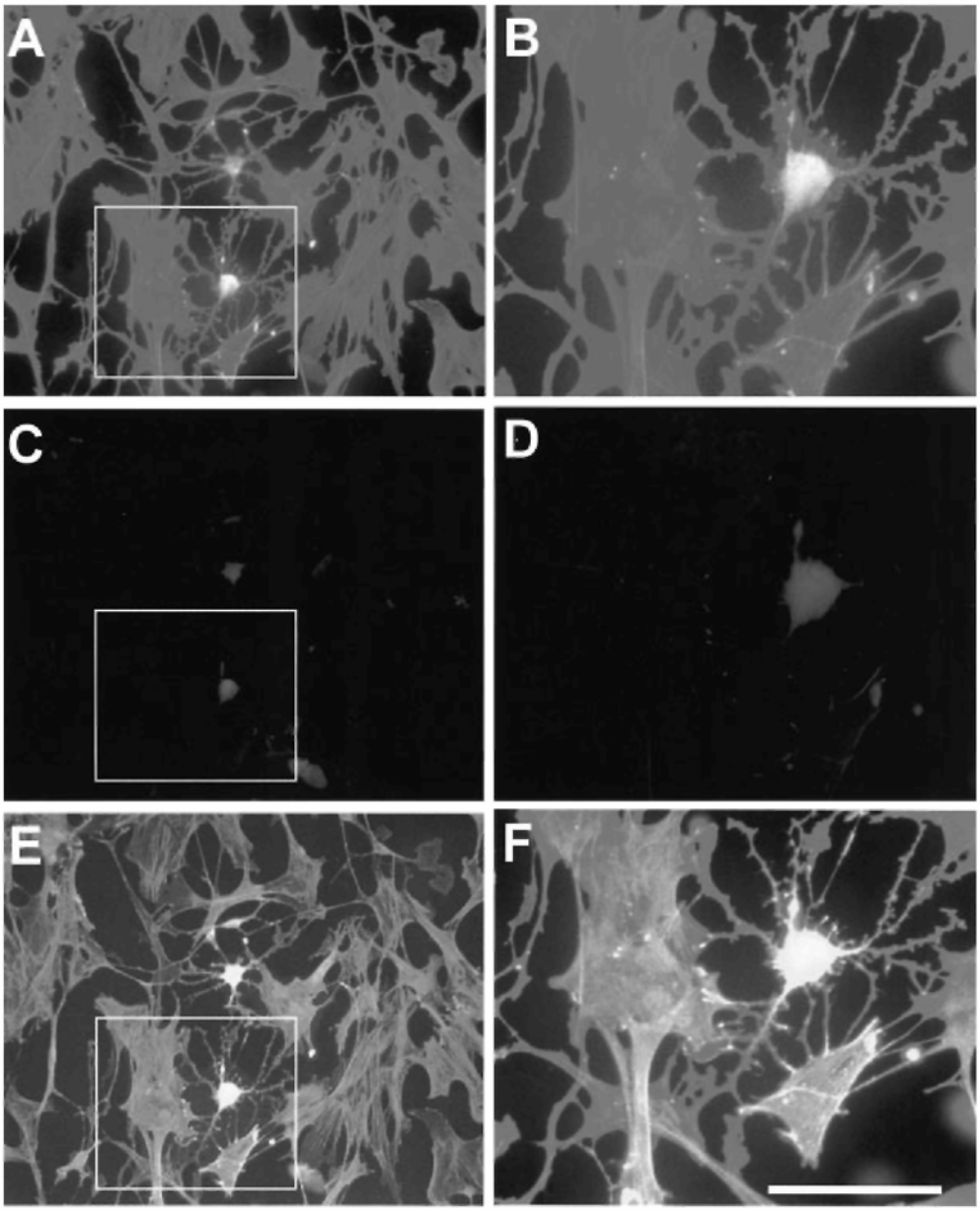

Discussion

Our results suggest that reversal of a given physiological process, namely pituicyte stellation, may involve events other than the mere reverse operation of the mechanism(s) that induced this process. We previously showed that adenosine-induced stellation is mediated by RhoA inhibition and is independent of Ca^{2+} (Rosso *et al.*, 2002; this study). Our present data indicate that reversal of stellation by AVP is independent of RhoA, involving instead Ca^{2+}-dependent activation of Cdc42. Nevertheless, it should be mentioned that RhoA activation, e.g. with LPA treatment, can also reverse cAMP- (Manning & Sontheimer, 1997) or adenosine-induced stellation (our unpublished data). Interestingly, Manning & Sontheimer (1997) found that reversal of astrocyte stellation by LPA was Ca^{2+}-independent. This observation provides a further argument against RhoA involvement in AVP-mediated reversal, for which we did observe Ca^{2+} dependence.

Whether the RhoA and Cdc42 pathways act in parallel or in series is a relevant question here, inasmuch as there are indications that RhoA could act downstream of Cdc42 (reviewed in Hall, 1998). Nevertheless, the idea of parallel pathways is more consistent with our data, based on the observation that AVP activates Cdc42 independently of RhoA and reverses C3-induced stellation. This idea is supported further by the fact that Cdc42 inhibition by NWASP-GBD does not induce stellation whereas RhoA inhibition does. However, another possibility is that both pathways are independent but converge at a common downstream effector. Lysophosphatidic acid failed to block C3-induced stellation but did block stellation induced by Y-27632, an inhibitor of the RhoA-specific effector p160Rho kinase. This suggests that RhoA could control another effector besides p160Rho kinase, which is consistent with the fact that small GTPases can activate multiple downstream targets (Hall, 1998). Thus, inhibition of p160Rho kinase could be both necessary and sufficient for induction of stellation, whereas activation of another, perhaps yet unknown, effector common to RhoA and Cdc42 would be able to reverse stellation. Dong *et al.* (1998, 2002) reported that activation of RhoA or Cdc42 can block cAMP-mediated stellation of SH-EP neuroblastoma cells. The two GTPases had opposite effects on actin stress fibres but similarly sustained focal adhesion complexes, which is not inconsistent with the above hypotheses.

To our knowledge, the finding that Ca^{2+} controls the activity of Cdc42 is novel. The mechanisms involved in the Ca^{2+} sensitivity of Cdc42 could be related to the phosphorylation state of the GTPase (Forget *et al.,* 2002), which might be driven by Ca^{2+}-dependent kinases and/or phosphatases. By contrast, our results for adenosine-induced stellation imply that Ca^{2+} is irrelevant to RhoA inactivation; moreover, the fact that LPA-induced reversal of stellation is Ca^{2+}-insensitive (Manning & Sontheimer, 1997) calls for the same conclusion regarding RhoA activation. This, together with the likely mutual independence of RhoA and Cdc42 as discussed above, suggests that a Ca^{2+} signal could provide a switch for selective activation of Cdc42. However, an absolute Ca^{2+} requirement for Cdc42 activation is difficult to reconcile with the fact that depletion of both intra- and extracellular Ca^{2+} only blocked ~70% of the action of AVP (see Fig. 5). In other words, it is not clear how 30% of the cells reverted to their basal shape in the absence of any Ca^{2+} signal. One possible explanation is that Ca^{2+} is only a permissive factor, and that the level of active Cdc42 remaining in its absence is sufficient to drive a certain amount of shape change. Indeed, we used a relatively high concentration (10^{-8} M) of AVP for both morphological (Fig. 5) and pull-down (Fig. 7) experiments. However, there is no possible direct, quantitative comparison, in our experimental conditions, between the level of activated Cdc42 with or without Ca^{2+}, and that necessary for stellation reversal.

Regarding Ca^{2+}-dependent reversal of stellation in general, it is worth noting that Tas & Koschel (1998) obtained results similar to ours with C6 rat glioma cells. They found that depletion of extracellular or intracellular Ca^{2+} strongly (but incompletely) antagonized sphingosine-1-phosphate-mediated reversal of β-adrenergic stellation. Unfortunately, they were unable to test the effect of extracellular and intracellular Ca^{2+} depletion because of the cell toxicity of the procedure. These authors concluded that Ca^{2+} is essential but not sufficient for reversal of stellation as the latter cannot be achieved by 'artificially' increasing the divalent cation, e.g. with ionomycin. Our finding that the inhibitory effects of blocking the $[Ca^{2+}]_i$ and $[Ca^{2+}]_e$ signals are not additive could be explained by the fact that only the $[Ca^{2+}]_e$ signal is important in reversal of stellation. In this respect, BAPTA, which is a fast Ca^{2+} chelator, might quickly buffer Ca^{2+} influx, thereby blocking reversal of stellation to the same extent as $[Ca^{2+}]_e$ depletion. This view is consistent with the similarities between the dose-response curves for AVP-induced reversal of stellation and generation of a sustained Ca^{2+} signal. Most notably, these curves have identical IC/EC_{50} values, and they reach a plateau at about 1 nM agonist, a concentration that involves little of the transient Ca^{2+} signal. The latter might fulfill a function other than regulation of morphological changes (Hatton *et al.,* 1992).

The finding that reversal of stellation is Ca^{2+}-dependent might help resolve another issue. During our previous work (Rosso *et al.,* 2002), we found that adenosine can induce a $[Ca^{2+}]_i$ signal in a limited proportion of pituicytes. This effect occurs especially at low concentrations of agonist, and is independent of the A_1 receptor (the one involved in purinergic stellation) as it is not blocked by DPCPX, an Al antagonist (Peteri-Brunbäck *et al,* 2002). This could explain two observations that we make routinely. First, 100% stellation is very rarely obtained with saturating concentrations of adenosine; 70-80% is most commonly observed. Second, the cells that do become stellate spontaneously revert within about 2 h in the presence of agonist. A plausible scenario is that nonresponsive cells have a high proportion of non-A1 receptors, which, once activated, will prevent stellation via $[Ca^{2+}]_i$ increase and subsequent stimulation of Cdc42. Stellate cells, by contrast, might progressively revert as the balance between activation of A_1 and non-A1 receptors moves in favour of the latter, perhaps as a function of agonist concentration.

To conclude, our data show that physiological concentrations of AVP can reverse pituicyte stellation through Cdc42 activation. Because stellation has been hypothesized as facilitating hormone release (Hatton, 1988), AVP

might constitute a feedback regulator of its own output. Our finding that much higher concentrations of OXT are necessary to yield the same effects as AVP is consistent with the fact that vasopressor and antidiuretic activities of OXT are 100-fold lower than those of AVP (Manning *et al.,* 1981).

Acknowledgements

We are grateful to Drs Patrice Boquet, Akiko Yoshimura, Claudine Serradeil-Le Gal, Alan Hall, Pierre Roux and Maurice Manning for the gift of their compounds. V.V.C., C.D. and E.V.O.S. acknowledge financial support from the Association pour la Recherche contre le Cancer (ARC).

Abbreviations

$[Ca^{2+}]_i$, intracellular Ca^{2+}; $[Ca^{2+}]_e$, extracellular Ca^{2+}; AVP, arginine-vasopressine; CRIB, Cdc42/Rac interactive binding domain; DPCPX, 1,3-dipropyl-8-cyclopentylxanthine; GST, glutathione-S-transferase; LPA, lysophosphatidic acid; MAPK, mitogen-activated protein kinase; OXT, oxytocin; RBD, RhoA binding domain; WASP, Wiscott-Aldrich syndrome protein; GBD, Cdc42 GTPase binding domain.

References

Andrès, M., Trueba, M. & Guillon, G. (2002) Pharmacological characterization of F-180: a selective human V_{1a} vasopressin receptor agonist of high affinity. *Br. J. Pharmacol,* 135, 1828-1836.

Bagrodia, S., Derijard, B., Davis, R.J. & Cerione, R.A. (1995) Cdc42 and PAK-mediated signaling leads to Jun kinase and p38 mitogen-activated protein kinase activation. *J. Biol. Chem.,* 270, 27995-27998.

Bicknell, R.J., Luckman, S.M., Inenaga, K., Mason, W.T. & Hatton, G.I. (1989) Beta-adrenergic and opioid receptors on pituicytes cultured from adult rat neurohypophysis: regulation of cell morphology. *Brain Res. Bull.,* 22, 379-388.

Chardin, P., Boquet, P., Madaule, P., Popoff, M.R., Rubin, E.J. & Gill, D.M. (1989) The mammalian G protein rhoC is ADP-ribosylated by Clostridium botulinum exoenzyme C3 and affects actin microfilaments in Vero cells. *EMBO J.,* 8, 1087-1092.

Derick, S., Cheng, L.L., Stoev, S., Guillon, G. & Manning, M. (2001) Functional and pharmacological characterization of a specific vasopressin V1b agonist. In Theodosis, D.T. and Poulain, D.A. (organisers) *World Congress on Neurohypophysial Hormones,* September 8-12, 2001, INSERM U378, Bordeaux, France, 61. [Poster P1-15.]

Dong, J.M., Leung, T., Manser, E. & Lim, L. (1998) cAMP-induced morphological changes are counteracted by the activated RhoA small GTPase and the Rho kinase ROKα. *J. Biol. Chem.,* 273, 22554-22562.

Dong, J.M., Leung, T., Manser, E. & Lim, L. (2002) Cdc42 antagonizes inductive action of cAMP on cell shape, via effects of the myotonic dystrophy kinase-related Cdc42-binding kinase (MRCK) on myosin light chain phosphorylation. *Eur. J. Cell Biol,* 81, 231-242.

Elands, J., Barberis, C, Jard, S., Tribollet, E., Dreifuss, J.J., Bankowski, K., Manning, M. & Sawyer, W.H. (1988) ^{125}I-labelled d $(CH_2)_5$[Tyr (Me) ^{2},Thr^4,Tyr-NH29]OVT: a selective oxytocin receptor ligand. *Eur. J. Pharmacol,* 147, 197-207.

Forget, M.A., Desrosiers, R.R., Gingras, D. & Beliveau, R. (2002) Phosphorylation states of Cdc42 and RhoA regulate their interactions with Rho GDP dissociation inhibitor and their extraction from biological membranes. *Biochem. J.,* 361, 243-254.

Gratzl, M., Torp-Pedersen, C, Daertt, D., Treiman, M. & Thorn, N.A. (1980) Isolation and characterization of secretory vesicles from bovine neurohypophyses. *Hoppe Seylers Z. Physiol Chem.,* 361, 1615-1628.

Hall, A. (1998) Rho GTPases and the actin cytoskeleton. *Science, 219,* 509-514.

Hatton, G.I. (1988) Pituicytes, glia and control of terminal secretion. *J. Exp. Biol,* 139, 67-79.

Hatton, G.I. (1999) Astroglial modulation of neurotransmitter/peptide release from the neurohypophysis: present status. *J. Chem. Neuroanat.,* 16, 203- 222.

Hatton, G.I., Bicknell, R.J., Hoyland, J., Bunting, R. & Mason, W.T. (1992) Arginine vasopressin mobilises intracellular calcium via V_1-receptor activation in astrocytes (pituicytes) cultured from adult rat neural lobes. *Brain Res.,* 588, 75-83.

Jung, S., Strotmann, R., Schultz, G. & Plant, T.D. (2002) TRPC6 is a candidate channel involved in receptor-stimulated cation currents in A7r5 smooth muscle cells. *Am. J. Physiol. Cell. Physiol,* 282, C347-C359.

Lim, L., Manser, E., Leung, T. & Hall, C. (1996) Regulation of phosphorylation pathways by p21 GTPases. The p21 Ras-related Rho subfamily and its role in phosphorylation signalling pathways. *Eur. J. Biochem.,* 242, 171-185.

Machesky, L.M. & Hall, A. (1996) Rho: a connection between membrane receptor signalling and the cytoskeleton. *Trends Cell. Biol,* 6, 304-310.

Manning, M., Grzonka, Z. & Sawyer, W.H. (1981) Synthesis of posterior pituitary hormones and hormone analogues. In Beardwell, C. & Robertson, G.L. (eds), *The Pituitary.* Butterworths, London, pp. 265-296.

Manning, T.J. Jr & Sontheimer, H. (1997) Bovine serum albumin and lysophosphatidic acid stimulate calcium mobilization and reversal of cAMP-induced stellation in rat spinal cord astrocytes. *Glia,* 20, 163-172.

Miyata, S., Furuya, K., Nakai, S., Bun, H. & Kiyohara, T. (1999) Morphological plasticity and rearrangement of cytoskeletons in pituicytes cultured from adult rat neurohypophysis. *Neurosci. Res.,* 33, 299-306.

Peteri-Brunbäck, B., Rosso, L. & Mienville, J.-M. (2002) The role of calcium signaling in the morphological plasticity of neurohypophysial astrocytes (pituicytes). *The 5th International Congress of Neuroendocrinology,* August 31 to September 4, 2002, Bristol, UK, International Nueroendocrine Federation, FC27.

Philips, A., Roux, P., Coulon, V., Bellanger, J.M., Vie, A., Vignais, M.L. & Blanchard, J.M. (2000) Differential effect of Rac and Cdc42 on p38 kinase activity and cell cycle progression of nonadherent primary mouse fibroblasts. *J. Biol. Chem.,* 275, 5911-5917.

Ramsell, K.D. & Cobbett, P. (1997) Serum uncouples elevation of cyclic adenosine monophosphate concentration from cyclic adenosine monophosphate dependent morphological changes exhibited by cultured pituicytes. *Neurosci. Lett.,* 226, 41-44.

Ren, X.D., Kiosses, W.B. & Schwartz, MA. (1999) Regulation of the small GTP-binding protein Rho by cell adhesion and the cytoskeleton. *EMBO J.,* 18, 578-585.

Rosso, L., Peteri-Brunbâck, B., Vouret-Craviari, V., Deroanne, C, Troadec, J.-D., Thirion, S., Van Obberghen-Schilling, E. & Mienville, J.-M. (2002) RhoA inhibition is a key step in pituicyte stellation induced by A_1-type adenosine receptor activation. *Glia,* 38, 351-362.

Serradeil-Le Gal, C. (1998) Nonpeptide antagonists for vasopressin receptors. Pharmacology of SR 121463A, a new potent and highly selective V2 receptor antagonist. *Adv. Exp. Med. Biol,* 449, 427-438.

Sperlágh, B., Mergl, Z., Jurányi, Z., Vizi, E.S. & Makara, G.B. (1999) Local regulation of vasopressin and oxytocin secretion by extracellular ATP in the isolated posterior lobe of the rat hypophysis. *J. Endocrinol,* 160, 343-350.

Tas, P.W. & Koschel, K. (1998) Sphingosine-1-phosphate induces a Ca^{2+} signal in primary rat astrocytes and a Ca^{2+} signal and shape changes in C6 rat glioma cells. *J. Neurosci. Res.,* 52, 427-434.

Theodosis, D.T. & Macvicar, B. (1996) Neurone-glia interactions in the hypothalamus and pituitary. *Trends Neurosci.,* 19, 363-367.

Thirion, S., Troadec, J.-D. & Nicaise, G. (1996) Cytochemical localization of ecto-ATPases in rat neurohypophysis. *J. Histochem. Cytochem.,* 44, 103-111.

Troadec, J.-D., Thirion, S., Petturiti, D., Bohn, M.T. & Poujeol, P. (1999) ATP acting on P_{2Y} receptors triggers calcium mobilization in primary cultures of rat neurohypophysial astrocytes (pituicytes). *Pflügers Arch.,* 437, 745-753.

Uehata, M., Ishizaki, T., Satoh, H., Ono, T., Kawahara, T., Morishita, T., Tamakawa, H., Yamagami, K., Inui, J., Maekawa, M. & Narumiya, S. (1997) Calcium sensitization of smooth muscle mediated by a Rho- associated protein kinase in hypertension. *Nature,* 389, 990-994.

Zimmermann, H. (1994) Signalling via ATP in the nervous system. *Trends Neurosci.,* 17, 420-426.